P2.7 THE EFFECT OF CONTINENTAL AIR OUTBREAKS ON MARINE STRATOCUMULUS DRIZZLE FORMATION AND CLOUD BREAKUP

Lan Yi * Yefim Kogan David Mechem
Cooperative Institute for Mesoscale Meteorological Studies
University of Oklahoma, Norman, Oklahoma

1. INTRODUCTION

Through their effect on cloud microstructure and drizzle, cloud condensation nuclei (CCN) may significantly affect cloud geometry and persistence and, thus, play a significant role in the evolution of marine stratocumulus cloud layers as a whole. Over the oceans, CCN concentration and size distribution often exhibit considerable variability, especially due to outbreaks of continental air masses infrequently modified by anthropogenic pollution or dust events originated from deserts. In a stratocumulus topped boundary layer (STBL), strong temperature inversion prohibits mixing of the continental air mass aloft with the underlying clean marine air (Ansmann et al. 2001), resulting in elevated pollution layers (EPL) of high aerosol/CCN concentration above stratus or stratocumulus cloud layers. Based on measurements made during FIRE, ASTEX and ACE-1 field projects, a number of researchers (e.g., Hudson and Frisbie 1991; Frick and Hoppel 1993; Covert et al. 1996; Clarke et al. 1997; Hudson et al. 1998) have reported observations of such EPL in clean marine regions off the California coast and in the Pacific, Atlantic and the Southern Ocean.

Recent observations during the ACE-2 field program provided new cases of dramatic air pollution outbreaks which resulted in inhomogeneous vertical aerosol distribution over the ocean (e.g., Wood et al. 2000; Osborne et al. 2000; Putaud et al. 2000). Marked differences in the aerosol size distribution, composition, and state of mixing existed in the marine and continental air masses (Clarke et al. 1997). Fitzgerald (1991), for example, noted that in continental air masses the concentration of large and giant mode particles, such as nitrate or mineral dust, can occasionally equal the sea salt concentrations.

Given numerous observational evidence on the existence of EPL, we would like to ask the questions of: 1) how do different vertical profiles of CCN concentration affect the STBL microstructure and drizzle, and 2) how the latter are influenced by the CCN size composition in the EPL?

At present, very few studies have been made to address these questions. Jiang et al. (2001) investigated the influence of entrainment of CCN at cloud top on cloud evolution. They concluded that aerosol gradients across the top of the boundary layer can alter cloud microphysical properties and, in turn, cloud optical properties. Their study, however, did not consider the CCN size variation. Feingold et al. (1999) investigated the impact of giant CCN on drizzle formation in stratocumulus, however, the vertical variability of CCN particles has not been considered. In reality both CCN concentration and size distribution may vary across the STBL inversion.

In this study we investigate how the aerosol/CCN vertical variability in anthropogenically or naturally occurring EPL affects marine stratocumulus evolution and drizzle production. A set of numerical experiments is designed to conduct model runs with different CCN number and size distributions above and below the STBL inversion. The latter are compared with those that have constant CCN number and shape over the entire model domain. In addition we investigate the effect of wind shear across the inversion layer. The magnitude of the wind shear controls the rate at which continental CCN are entrained into the STBL, and, thus, the impact of pollution on STBL development.

2. MODEL AND EXPERIMENT DESCRIPTION

The study is based on the CIMMS LES model, which combines the 3-D dynamics with explicit (size-resolving) formulation of the liquid phase microphysical processes (Kogan et al 1995, Khairoutdinov and Kogan, 1999). The thermodynamic state is described in terms of the virtual liquid water potential temperature and the total water mixing ratio. The one and a half order turbulence closure is based on the prognostic equation for the subgrid scale turbulent kinetic energy. Cloud physics processes are treated based on the prediction equations for cloud particle spectra. The spectra of the basic cloud particles are taken into consideration: cloud condensation nuclei (19 bins) and cloud and drizzle drops (25 bins). The equations for particle size distribution functions include processes of advection, sedimentation, turbulent mixing, and individual microphysical processes of nucleation, condensation/evaporation and stochastic coagulation. The solar heating and longwave cooling rates at each grid point and at each time step are calculated using a computationally efficient broadband radiation package.

Earlier case studies showed that the model realistically reproduces dynamical, turbulence, radiative, and mi-

*Corresponding author address: Dr. Lan Yi, Cooperative Institute for Mesoscale Meteorological Studies, University of Oklahoma, Rm 1234 SEC, 100 E Boyd, Norman, OK 73019; e-mail: lanyi@ou.edu.

Table 1: Experiments simulating dust events with giant CCN initially at all levels (1G), above inversion (1GA), and below inversion (1GB). Similar notations are used for accumulation mode pollution (2M) and nucleation mode pollution (3S) events.

Event	All levels	Above inv.	Below inv.
Dust	1G	1GA	1GB
Pollu.	2M	2MA	2MB
Pollu.	3S	3SA	3SB

crophysical cloud parameters, including the position and magnitude of the maximum, as well as the overall shape of the observed droplet size distribution throughout the cloud (Khairoutdinov and Kogan, 1999).

Our control run (CR) experiment was initialized with an environmental sounding, large-scale subsidence, and surface flux parameters observed during ASTEX A209 clean maritime case. Cloud microphysics is determined by the concentration and activation spectrum of CCN that is spatially homogeneous. It is approximated by a lognormal distribution with a total count of 45 cm^{-3}, the median radius 0.1 μm, and a standard deviation 1.5 μm. Grid spacing is 75 m in the horizontal and 25 m in the vertical. Time steps for dynamics and microphysics are 4 seconds and 0.2 seconds, respectively.

We consider the elevated CCN concentrations above the inversion height to result from: a) heavy dust outbreaks with pollution particles at predominantly large and giant coarse modes, b) continental air intrusion with pollutant particles at the accumulation mode, c) fresh continental air intrusion with particles at the nucleation mode. Hence, three types of lognormal CCN spectra representative of the aforementioned cases are superimposed on the background marine CCN spectrum. Figure 1 shows the modified spectra to be used in the series of experiments listed in Table 1. The CCN vertical variability for simplicity is represented by a two-layered structure with the CCN concentration and size distribution above/below the inversion specified according to CCN values in respective continental air outbreak events, while below/above inversion we use the same background clean maritime CCN spectrum as in the control run. In the section below, the experiments describing continental air outbreaks above inversion at large and giant mode (1GA), accumulation mode (2MA), and nucleation mode (3SA) are compared with the control run, and with experiments

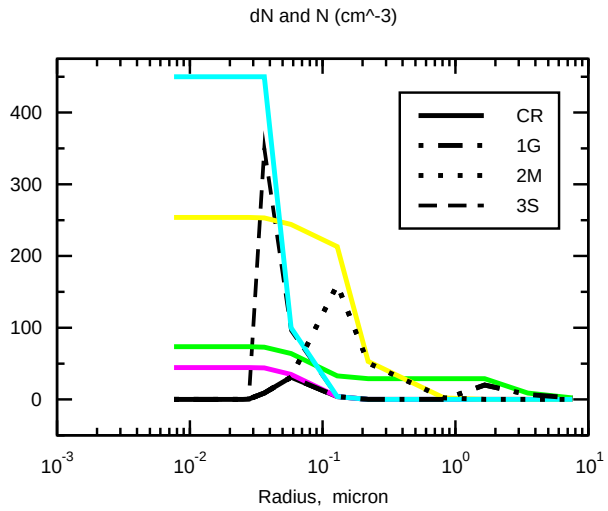

Figure 1: CCN spectra in the control run (CR) (solid line), in a dust event (1G) (dot-dashed line), in an accumulation mode dominated pollution event (2M) (dotted line), and in a nucleation mode dominated pollution event (3S) (dashed line). Corresponding cumulative spectra are also shown by color lines.

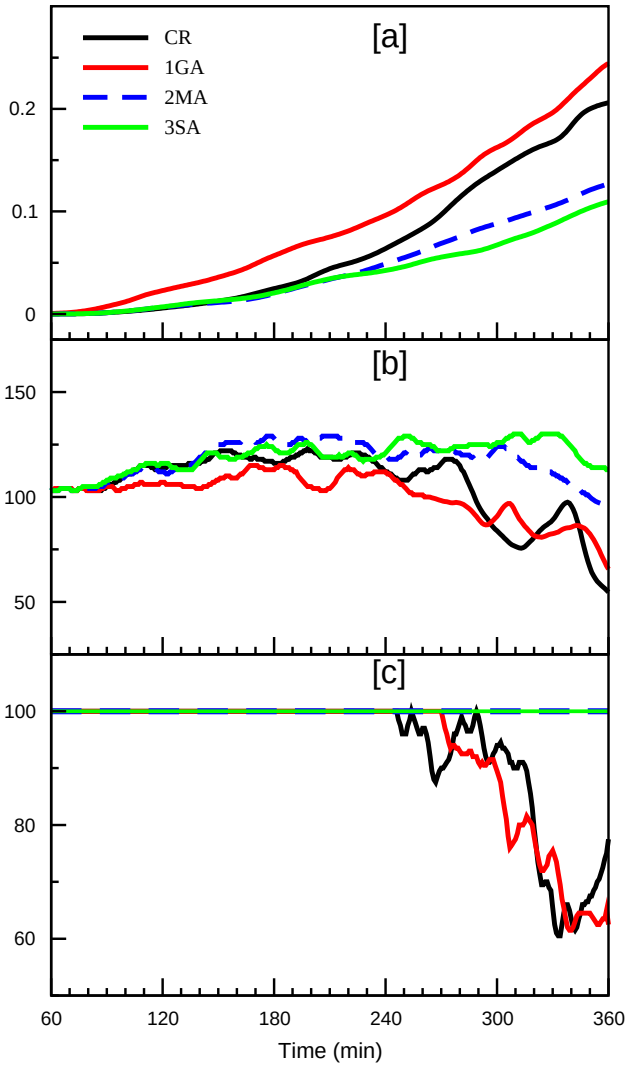

Figure 2: Time evolutions in various experiments of (a) cumulative subcloud layer mean drizzle (mm); (b) cloud liquid water path (g m^{-2}); (c) cloud cover(%).

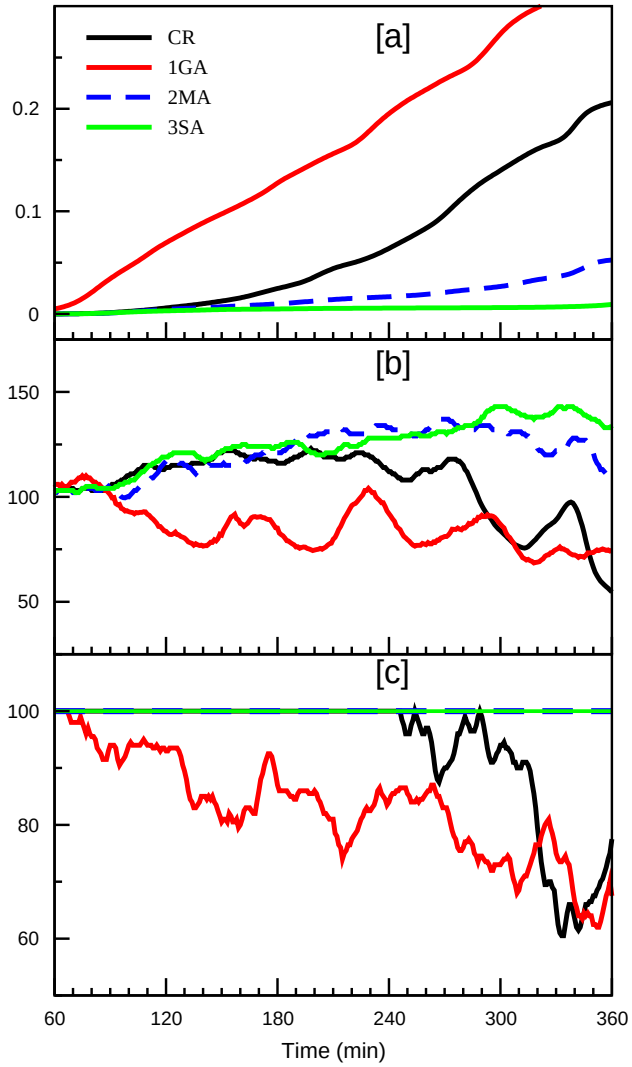

Figure 3: Same as Figure 2 except that continental CCN were supplied continuously in the simulations.

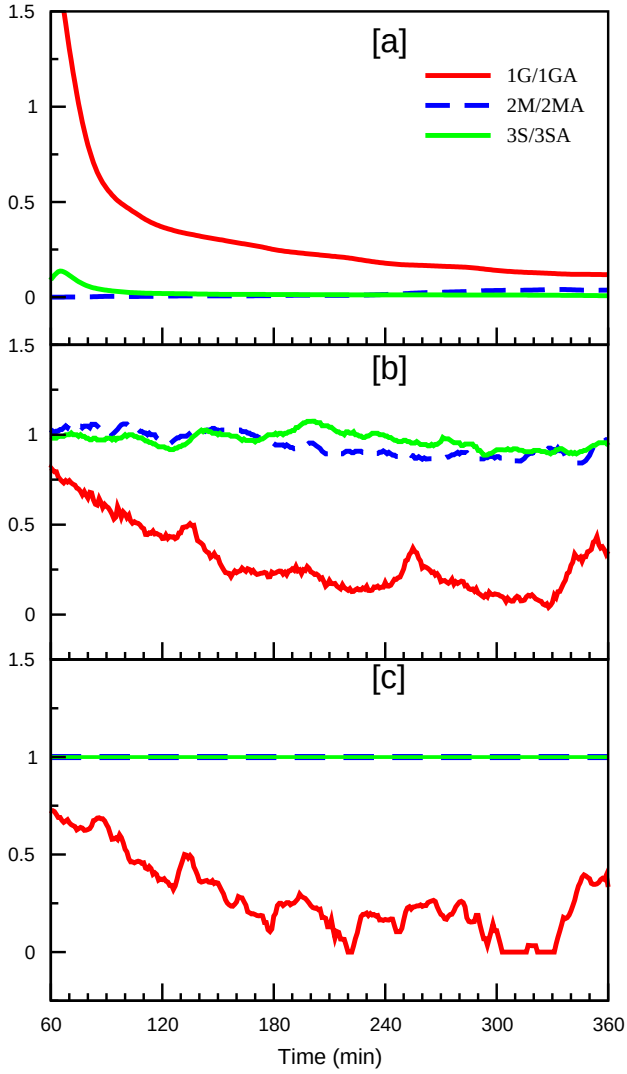

Figure 4: Same as Figure 3 except for the ratio of drizzle, LWP and cloud cover for cases 1G vs. 1GA, 2M vs. 2MA, and 3S vs. 3SA.

that apply corresponding CCN spectra at all model levels uniformly.

3. RESULTS

3.1 Effect of elevated polluted layers

Comparison of 1GA, 2MA, 3SA with CR in Figure 2 indicates that the effect of pollution above the inversion on drizzle and cloud properties depends strongly on the prevailing mode of CCN particles in the polluted air mass. In general, imposing large and giant mode pollutant particles above cloud top leads to more drizzle. In the dust case, the accumulated drizzle exceeded that in the control run, in spite of the fact that the CCN count (75 cm^{-3}) in this case was larger than in the CR clean maritime case (45 cm^{-3}). In cases 2MA and 3SA, where CCN of smaller sizes were added above inversion, the drizzle was suppressed to a lesser degree compared to experiments with similar size particles added at all levels in the domain (2M, 3S) (Figure not shown). As a rule, giant CCN in experiment 1GA tended to decrease cloud cover and cloud liquid water path, while smaller CCN seemed to have helped maintain cloud cover and cloud thickness (see Figure 2b and 2c).

To simulate polluted air masses from coastal surface sources which can be advected into the open ocean, although confined below the STBL inversion, we conducted three sensitivity experiments 1GB, 2MB and 3SB. The results of these experiments (not shown here) generally produce drizzle amounts and exhibit cloud structure similar to the experiments where additional polluted aerosol was added in the whole domain. The "below inversion experiments" produce less intensive drizzle and breakup later than the "above inversion experiments". The giant mode case (1GB) obviously produced more drizzle compared to the fine mode cases 2MB and 3SB, similar to the differ-

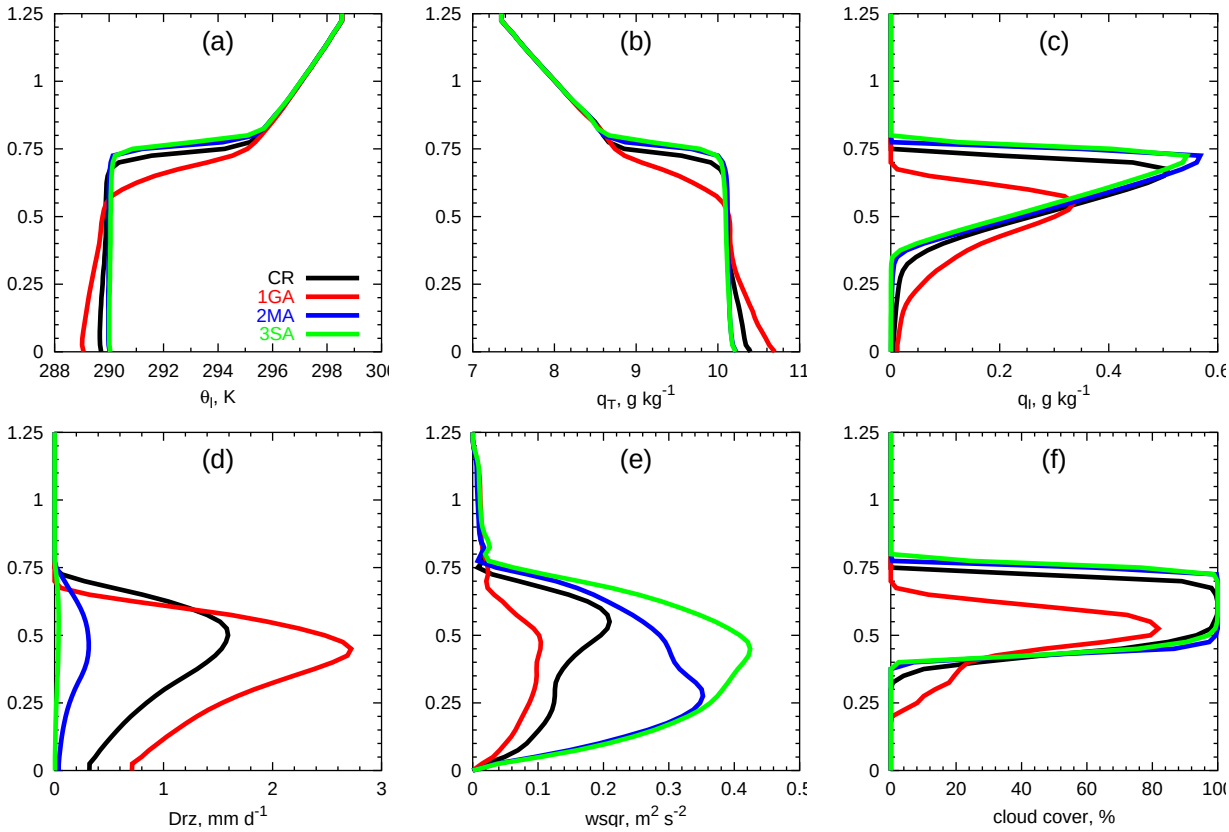

Figure 5: Mean vertical profiles averaged at 3-4hr into the simulations of (a) liquid water potential temperature, (b) total water, (c) liquid water, (d) drizzle rate, (e) vertical velocity variance, (f) cloud cover. Different colors represent different experiments. Y-axis is the height in km.

ences between 1GA versus 2MA and 3SA.

One of the implications of these results is that aerosol indirect effect depends not only on the total aerosol load, but also on the vertical variation of the latter and the size of the dominant aerosol particles.

3.2 Effect of wind-shear controlled pollution source persistence

Depending on wind conditions above and below the STBL inversion, the advection velocity of the EPL may be equal or different from that of the cloud layer. In the first case the cloud is seeded by CCN from the same polluted air mass and this scenario is simulated best as an initial value problem. In the second case, the source of the CCN is continuously renewed. This process is best represented by imposing a fixed source of CCN at levels above the inversion. This study focused mainly on the sensitivity of STBL to various CCN sources; the effect of wind shear on thermodynamic parameters, including cloud top entrainment, has been left for future studies.

The results shown in Figure 2 represent the first case and were simulated as an initial value problem, i.e., cloud was in contact with the same air mass and the CCN entrained into the cloud were replaced not by a constant source of new CCN, but by turbulent mixing with CCN from the surrounding areas in the EPL.

Figure 3 shows drizzle and cloud evolution for the second case. The comparison with Figure 2 demonstrates that continuous supply of large/giant CCN produced pronounced effect on drizzle and cloud evolution. For fine mode CCN cases (2MA and 3SA vs. CR), the effect was opposite – the longer the exposure to external CCN, the less amount of drizzle was produced. This agrees with the common understanding that drizzle is suppressed in continental type air mass containing plenty of small CCN particles. The same observation as demonstrated by Figure 2 about the role of the vertical distribution of aerosol/CCN particles remains valid in the second case. This is especially true for large and giant CCN (cf., 1GA vs. CR in Figure 2 and 3), where more abundant CCN throughout the whole domain resulted in a twofold increase in drizzle and a rapid cloud breakup.

Figure 4 displays the ratio of drizzle, cloud liquid water path (LWP), and cloud cover for experiments 1G and 1GA, 2M and 2MA, 3S and 3SA. Compared to 2MA and 3SA, imposing external fine mode CCN particles continuously everywhere in the domain throughout the model run time (2M, 3S) completely eliminated drizzle, maintained 100% cloud cover, and had a negligible effect on cloud thickness. For the experiment (1G) that had large/giant CCN added at all levels constantly, drizzle was greatly intensified in

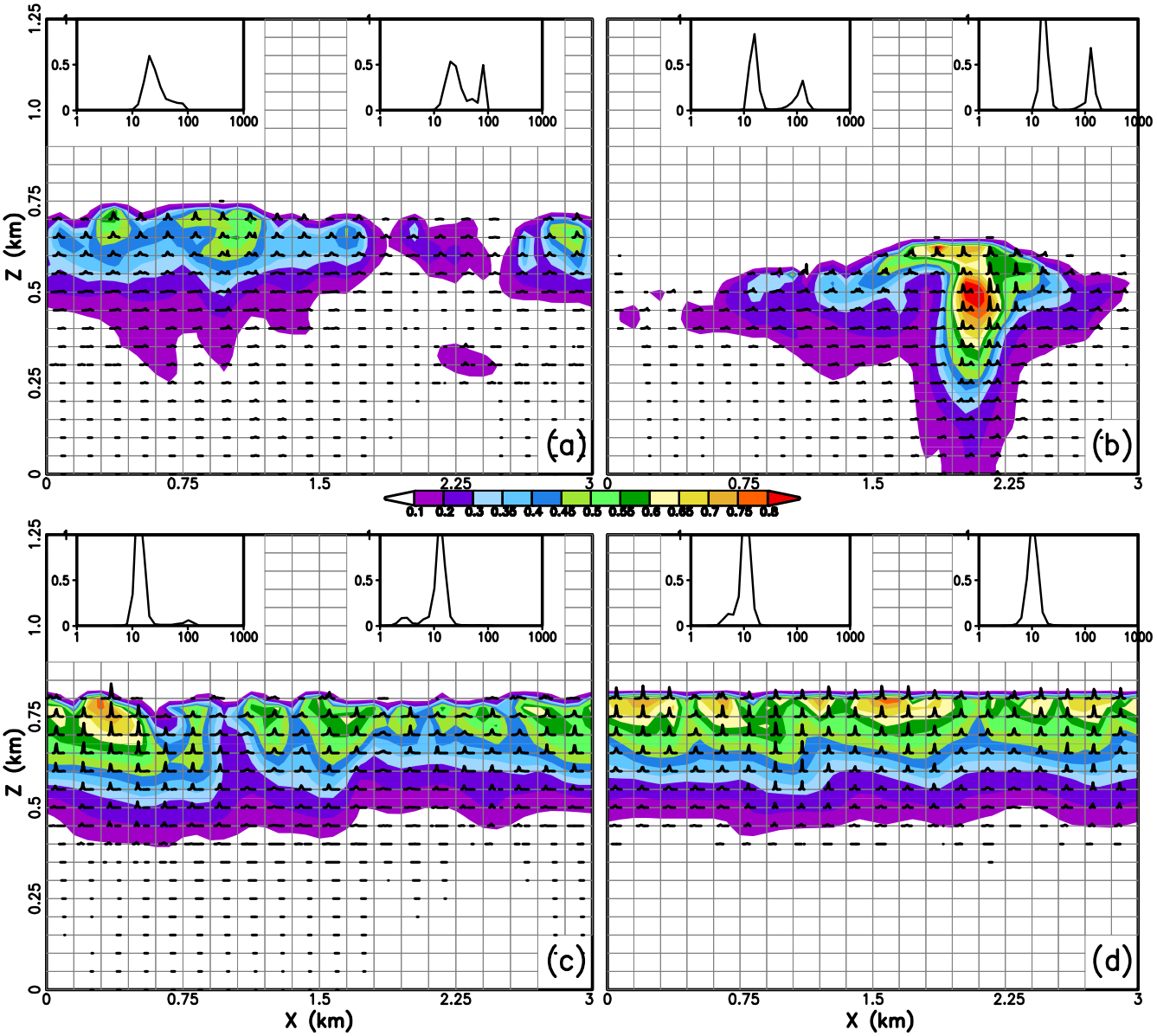

Figure 6: Cloud droplet mass distributions (plotted every other grid) in the x-z cross-section at 5 hr for experiments (a) CR; (b) 1GA; (c) 2MA; (d) 3SA. Cases (b)-(d) had constant CCN supply. Shadings depict cloud liquid water content (g kg^{-1}). Spectra zoomed out in each panel represent selected peak cloud droplet mass distributions, in which the x-axis is radius in μm, y-axis is mass function in g m^{-3} $(\log r)^{-1}$.

the initial stage (60-80 minutes), causing significant thinning of the cloud and depletion of cloud water, resulting in an insignificant drizzle production at late stages of the simulation.

Figure 5 exhibits a general vertical structure of the STBL in cases CR, 1GA, 2MA and 3SA. It is closely related to Figure 6, which shows significant cloud droplet spectrum broadening as a consequence of seeding large and giant CCN from above the inversion (Figure 6b): the maximum cloud droplet radius was larger than 100 μm in the drizzle cores; while in the control run (Figure 6a) it was smaller than 100 μm; in 2MA, $<$ 30 μm (Figure 6c); and in 3SA, $<$ 20 μm (Figure 6d). Panels (a)-(f) in Figure 5 together with Figure 6 demonstrate that seeding of the cloud layer by large and giant CCN (1GA) significantly enhanced the drizzle efficiency, leading to accelerated stratocumulus breakup, decoupling and stratification of the subcloud layer, attenuated turbulence, larger undulation of cloud top, and widening of the entrainment zone. On the other hand, enhancing the accumulation mode or nucleation mode CCN in EPL (2MA and 3SA) produced more cloud droplets and less drizzle, preserving the solid stratocumulus cloud deck, maintaining turbulent motions that lead to a rising cloud layer and inversion. The dynamical response of the boundary layer to changes in drizzle intensity induced by the EPL effect is in agreement

with previous studies (e.g., Stevens et al. 1998).

4. CONCLUSIONS

We investigated the role of CCN that have different vertical profiles, as well as size distribution, in marine stratocumulus drizzle production and cloud dynamical structure. Based on LES model with explicit microphysics, we simulated polluted continental air outbreaks characterized by three different CCN size modes (giant, accumulation, and nucleation). Our major conclusions are as follows,

(1) In order to quantify the aerosol indirect effect, it is important to take into account not only the total aerosol particle load, but also its vertical variation in the polluted continental air masses, the size of the dominant particles, and the wind shear across the inversion that controls the strength of the polluted CCN source.

(2) Enhanced large and giant CCN descending into the cloud layer from the EPL above the inversion significantly enhanced drizzle efficiency through cloud droplet spectrum broadening, leading to accelerated stratocumulus breakup, decoupling of the sub cloud layer, attenuated turbulence, larger undulation of cloud top, and widening of the entrainment zone.

(3) In a marine air mass modified by continental air characterized by fine mode CCN, precipitation was suppressed. The suppression was less if the pollutant particles (in accumulation or nucleation mode) were seeded from an EPL above the inversion.

(4) The feedbacks between the continental aerosol forcing and drizzle efficiency, positive for large and giant particles and negative for accumulation and nucleation mode particles, were enhanced in the presence of wind shear.

The above conclusions emphasize the need for a detailed aerosol/CCN consideration in LES models. Accurate prediction of stratocumulus drizzle and radiative properties, as well as STBL development, requires knowledge of the anthropogenic or natural aerosol vertical distribution, its size composition, and the wind shear across the inversion level on a broad scale.

ACKNOWLEDGMENTS

This work was supported by ONR-DOD Grants N00014-96-1-0687 and N00014-96-1-1112. Dr. Graham Feingold at NOAA Environmental Technology Laboratory provided helpful references and discussions.

REFERENCES

Ansmann, A., F. Wagner, D. Althausen, D. Muller, A. Herber, and U. Wandinger, 2001: European pollution outbreaks during ACE 2: lofted aerosol plumes observed with Raman lidar at the Portuguese coast. *J. Geophys. Res.*, **106**, 20725-20733.

Clarke, A. D., T. Uehara, and J. N. Porter, 1997: Atmospheric nuclei and related aerosol fields over the Atlantic: Clean subsiding air and continental pollution during ASTEX. *J. Geophys. Res.*, **102**, 25281-25292.

Covert, D. S., V. N. Kapustin, T. S. Bates, and P. K. Quinn, 1996: Physical properties of marine boundary layer aerosol particles of the mid-Pacific in relation to sources and meteorological transport. *J. Geophys. Res.*, **101**, 6919-6930.

Feingold, G., W. R. Cotton, S. M. Kreidenweis, and J. T. Davis, 1999: Impact of giant cloud condensation nuclei on drizzle formation in marine stratocumulus: Implications for cloud radiative properties. *J. Atmos. Sci.*, **56**, 4100-4117.

Fitzgerald, J. W., 1991: Marine aerosols: A review. *Atmos. Environ.*, **25A**, 533-545.

Frick, G. M., and W. A. Hoppel, 1993: Airship measurements of aerosol size distributions, cloud droplet spectra, and trace gas concentrations in the marine boundary layer. *Bulletin of A. M. S.*, **74**, 2195-2202.

Hudson, J. G., and P. R. Frisbie, 1991: Cloud condensation nuclei near marine stratus. *J. Geophys. Res.*, **96**, 20795-20808.

Hudson, J. G., Y. H. Xie, and S. S. Yum, 1998: Vertical distributions of cloud condensation nuclei spectra over the summertime Southern Ocean. *J. Geophys. Res.*, **103**, 16609-16624.

Jiang, H., G. Feingold, W. R. Cotton, and P. G. Duynkerke, 2001: Large-eddy simulations of entrainment of cloud condensation nuclei into the Arctic boundary layer: May 18, 1998, FIRE/SHEBA case study. *J. Geophys. Res.*, **106**, 15113-15122.

Khairoutdinov, M. F., and Y. L. Kogan, 1999: A large-eddy simulation model with explicit microphysics: Validation against aircraft observations of a stratocumulus-topped boundary layer. *J. Atmos. Sci.*, **56**, 2115-2131.

Kogan, Y. L., M. P. Khairoutdinov, D. K. Lilly, Z. N. Kogan and Q. Liu, 1995: Modeling of stratocumulus cloud layers in a large eddy simulation model with explicit microphysics. *J. Atmos. Sci.*, **52**, 2923-2940.

Osborne, S. M., D. W. Johnson, R. Wood, B. J. Bandy, M. O. Andreae, C. D. O'Dowd, P. Glantz, K. J. Noone, C. Gerbig, J. Rudolph, T. S. Bates and P. K. Quinn, 2000: Evolution of the aerosol, cloud and boundary-layer dynamic and thermodynamic characteristics during the 2nd Lagrangian experiment of ACE-2. *Tellus*, **52B**, 375-400.

Putaud, J. -P., R. Van Dingenen, M. Mangoni, A. Virkkula, F. Raes, H. Maring, J. M. Prospero, E. Swietlicki, O. H. Berg, et al., 2000: Chemical mass closure and assessment of the origin of the submicron aerosol in the marine boundary layer and the free troposphere at Tenerife during ACE-2. *Tellus*, **52B**, 141-168.

Stevens, B., W. R. Cotton, G. Feingold, and C.-H. Moeng, 1998: Large-eddy simulations of strongly precipitating, shallow, stratocumulus-topped boundary layers. *J. Atmos. Sci.*, **55**, 3616-3638.

Wood, R., D. Johnson, S. Osborne, M. O. Andreae, B. Bandy, T. S. Bates, C. O'Dowd, et al., 2000: Boundary layer and aerosol evolution during the 3rd Lagrangian experiment of ACE-2. *Tellus*, **52B**, 401-422.